Ultra Wide Band Surveillance Radar

AESS Distinguished Lecture Series

21 March 2023

Dr. Mark E Davis
IEEE Life Fellow
AESS President (2022-2023)
medavis@ieee.org
Clinton NY USA

Join AESS!

Go to http://ieee-aess.org/ and click on 'membership' to join today!

- The AESS is the only professional society dealing with total integrated electronic systems and the enabling technologies. AESS pioneered large-scale integrated interoperable systems. We interact with all technical societies and organizations. Additional Benefits include:
  - Panel and committee membership
  - Conferences and symposia
  - Present papers
  - Prizes and awards for technical accomplishments
  - Benefit from our Distinguished Lecturer Series
  - All members receive Aerospace and Electronic Systems magazine and a discount on Transactions.

Outline - AESS Distinguished Lecture

Objective: Provide A History Of Airborne Surveillance Radars, And Project Advanced Capabilities With Emerging Technologies

1. History Of Airborne Surveillance Systems
2. Ultra Wideband Antennas
3. Ultra Wideband Synthetic Aperture Radar Processing
4. Interferometric Radar Modes
5. Ultra Wideband Ground Moving Target Detection
6. UWB Multimode Operation (SAR and GMTI)
7. References

Ultra Wide Band Radar Objectives

- Ultra Wide Band (UWB) Radar Has Many Applications:
  - Significant Improvements In Range And Cross Range Resolution For Discrimination/Characterization Of Objects From Clutter
  - Foliage Penetration – Detection and Characterization of Objects Under Dense Foliage
  - Ground Penetration – Detection of Buried Objects And Unexploded Ordinance
  - Land Use/ Land Characterization For Earth Observation
- Key Technology Advances Have Facilitated These Objectives :
  - Global Positioning Systems, Solid State Transmitters, High Dynamic Range Digitization, High Performance Computation
- Commercialization Of Digital/Personal Communications Has Significantly Complicated Frequency Use Licensing
  - Stringent Requirements On Spectrum Use And Spectral Purity

Advancing Technology for Humanity

[davi21]

Multiple Aperture Surveillance Radar (MASR)

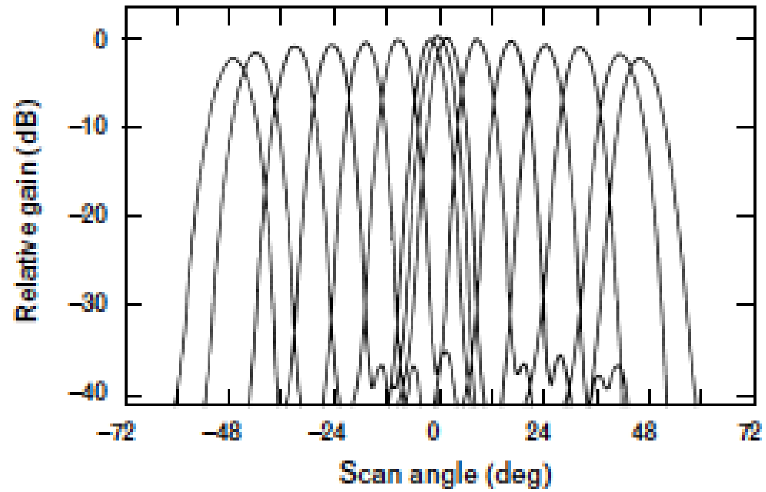

- Experimental GMTI Radar System – MIT Lincoln Laboratory
- L-Band With Unique Multiple Channel Phased Array Architecture
  - 42 Vertical Columns Of Low Sidelobe Radiators
  - Excellent Phase Match Switching Between Sections Of Antenna
- Achieved > 46 dB Clutter Cancellation
  - Switching Between Along Track Elements Pulse-to-Pulse
  - Ideal Displaced Phase Center Antenna (DPCA) for Stationary Clutter Cancellation

[brya00]

Hostile Weapons Locator Systems (HOWLS)

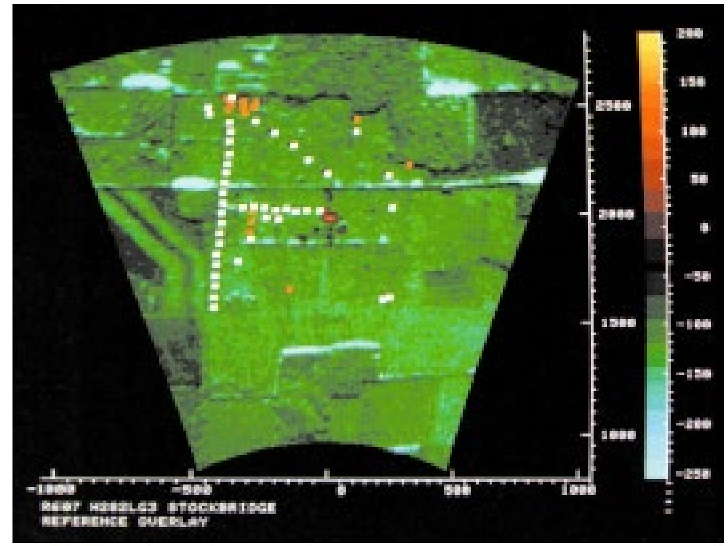

- Early Battlefield Surveillance Radar Intended For Remotely Piloted Vehicles (RPV)
- Ku Band Electronically Scanned Antenna With Coherent Multimode Operation
    - Ground Moving Target Indication Against Tracked And Wheeled Vehicles
    - Detection And Characterization Of Artillery Pieces
    - Early Doppler Beam Sharpened Mapping For Stationary Vehicles And Structures
- Data Link To Ground-base Signal Processing And Data Recording System

[brya00]

GeoSAR Interferometric Mapping System

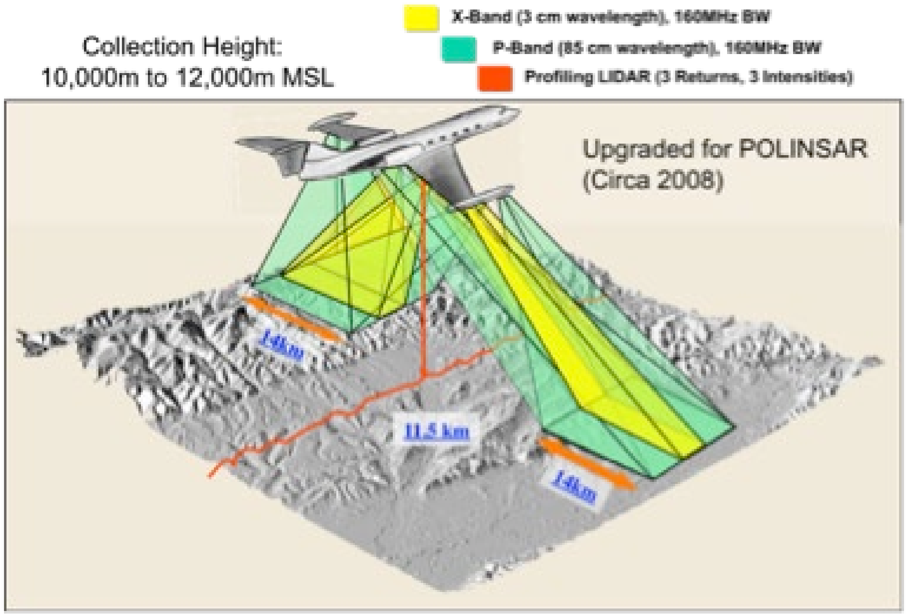

- Designed By NASA Jet Propulsion Laboratory For Bald Earth Mapping Under Foliage, & Characterization Of Dense Forests
- Funded by DARPA Under Dual Use “Other Transactions” Authority
- Dual Frequency For Mapping Tops and Near-bottom of Forests
- Continuous Operation World-wide 2003 - 2015

System Characteristics

Parameter	X-band	P-band
DEM Height Accuracy*		
Single Swath	0.5–1.2m (Relative)	1–3m (Relative)
Mapping Mosaic	~1m (Absolute*)	~4m (Absolute*)
DEM Resolution	2.5–5m 3m Standard	2.5–5m 5m Standard
Planimetric Accuracy*	1.2m (Relative)	1.2m (Relative)
GPS/Lidar Control	~1m (Absolute*)	~4m (Absolute*)
Ground Swath Width	10–12km, Each side	10–12km, Each side
Radar Look Angles	25–60 deg	25–60 deg
Polarization	V V	2-sided: HH, HV 1-sided: HH, HV, VH, VV
Pixel Size (Draped)	1.0–5m Standard	1.0–5m Standard
* Terrain, Slope, and Foliage Density Dependent		

FOPEN

[hens07]

Airborne Surveillance Radar Progression to Ultra Wide Band

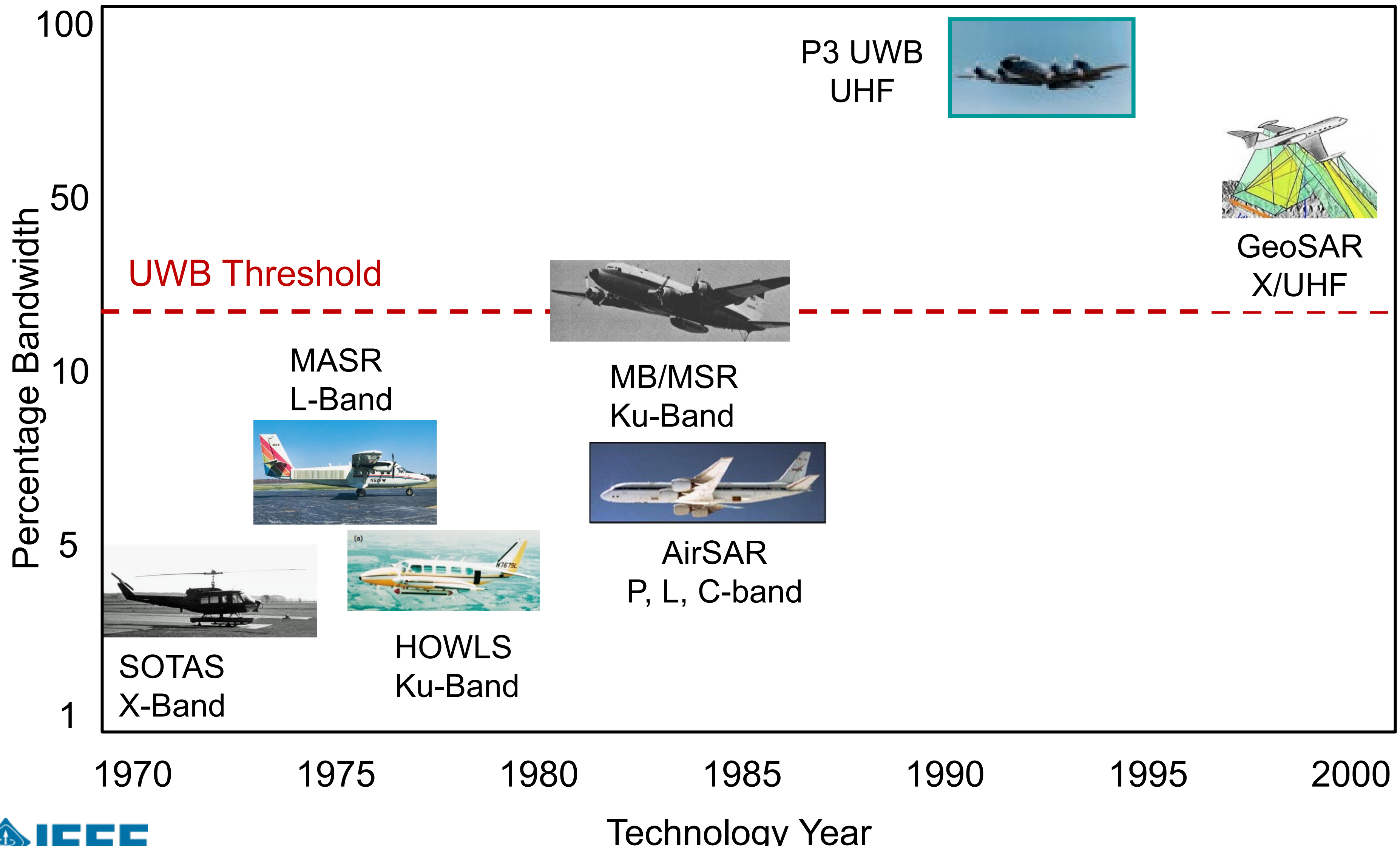

[davi21]

Comparison of UWB Surveillance Imagery

Aerial Photograph

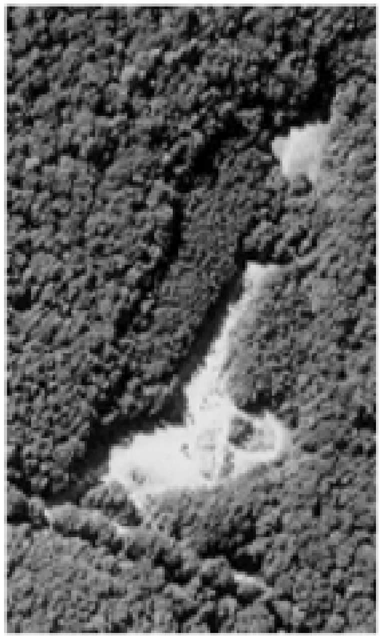

X-Band SAR

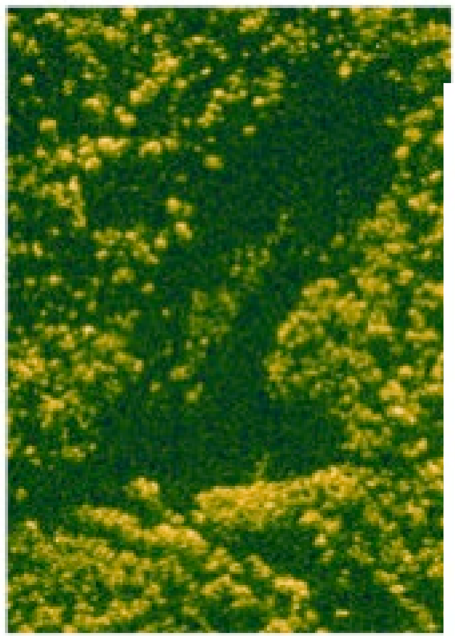

P-3 UWB UHF HH polarization

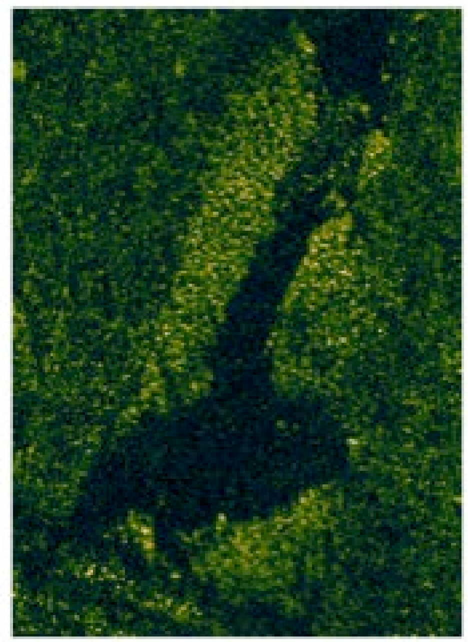

CARABAS VHF HH polarization

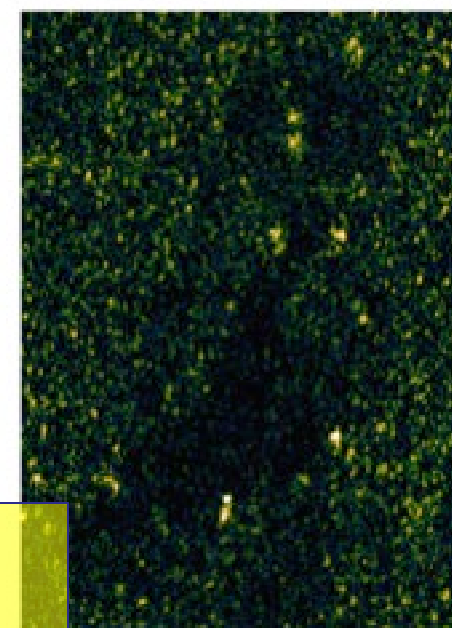

The Critical Tradeoff Is Between Resolution And Ability To Detect Targets In Dense Clutter

[davi11]

Phased Array Architectures

[bark76]

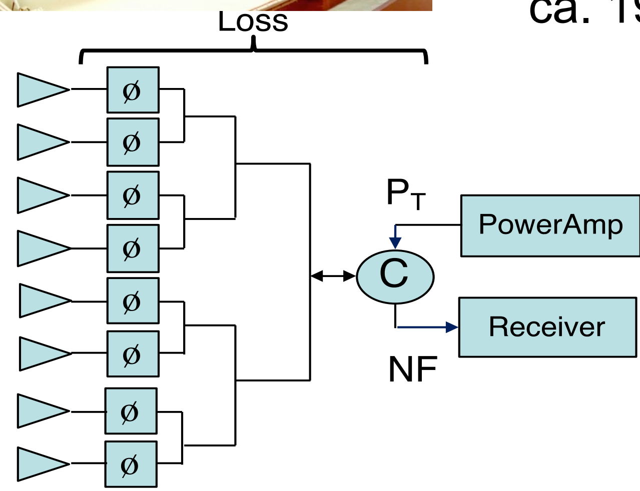

HOWLS
Passive Array
ca. 1977

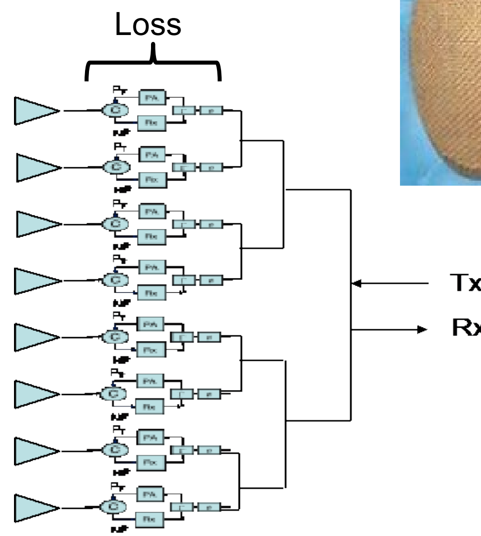

[manc08]

Thales
Active Array
ca. 2007

Passive Array

- + High Efficiency UWB Transmitter (Tube)
- + Reciprocal Tx and Rx Signal Paths
- \- High Loss After Tx, and Before Rx NF
- \- Tx Taper Through Feed Structure
- \- Very Heavy ESA Assembly

Active Array

- + Small Light Weight TR Modules
- + Low Loss After Tx, and Before Rx NF
- + Moderate Efficiency Solid State Tx
- \- Difficult Tx Taper For High Efficiency
- \- Tx and Rx Spectral Mismatch

MIMIC Program Introduced Single TR Chips by 2001 → UAV Applications

[davi21]

Wideband Electronic Scanned Array (ESA)

Wide Band Array Scanning

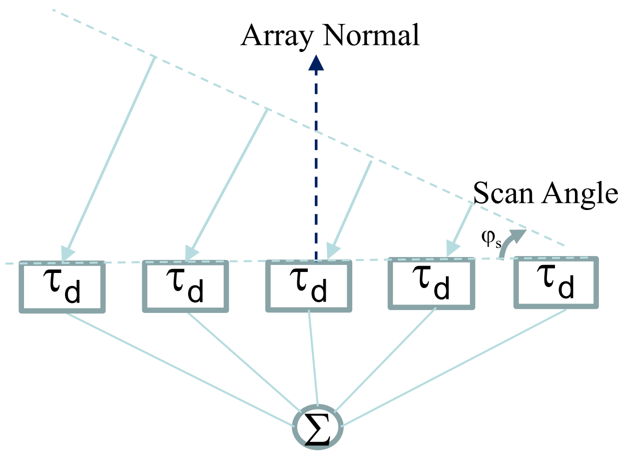

Linear Wide Band Array

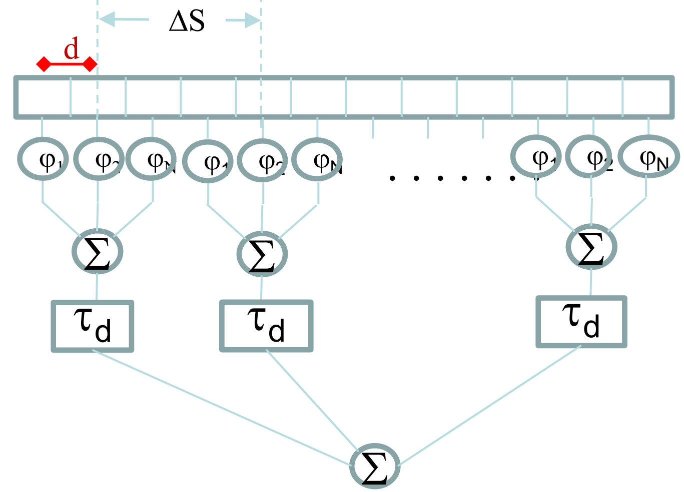

$$E(\varphi,\lambda) = \overbrace{\sum_{m=1}^{M} \exp\left[-j\frac{2\pi}{\lambda} m\, \Delta S(sin\varphi - sin\varphi_s)\right]}^{\text{Array Factor}} \overbrace{\sum_{n=1}^{N}\left[\exp(-j\, 2\pi\, n\, d\, (\frac{\sin\varphi}{\lambda} - \frac{\sin\varphi_s}{\lambda_0})\right]}^{\text{Sub Array Pattern}}$$

$$\tau_d = \frac{m\, d \sin\varphi_s}{c} \qquad d \leq \frac{\lambda}{(1 + |\sin\varphi_s|)} \qquad \theta_s = \frac{2\pi}{\lambda}\, n\, d \sin\varphi_s$$

Combination Of Phase And Time Delay Steering Required To Maintain Constant Phase Front Over Wide Bandwidth

[aalf13]

Digital Multiple Beam Forming

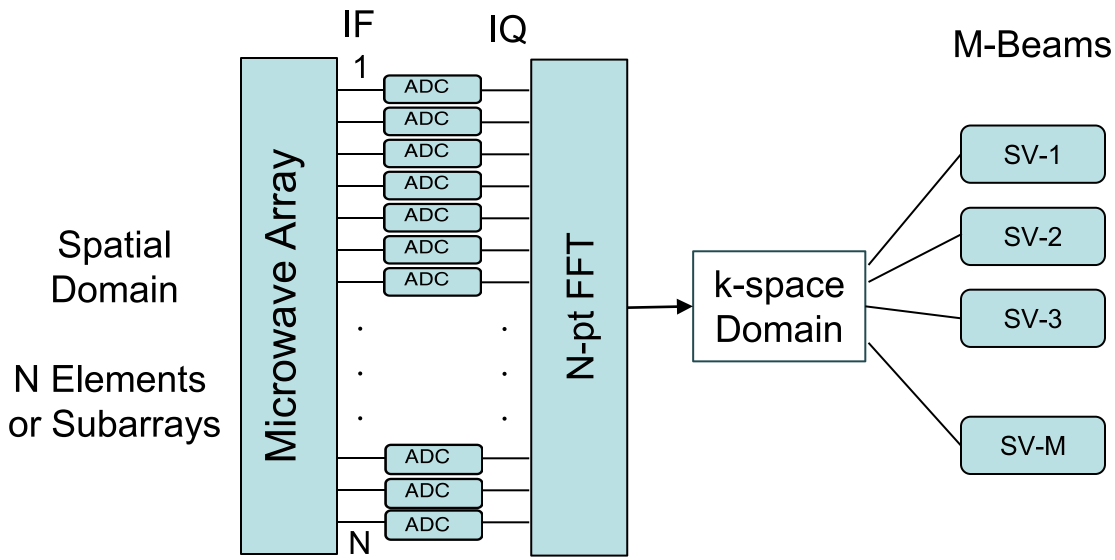

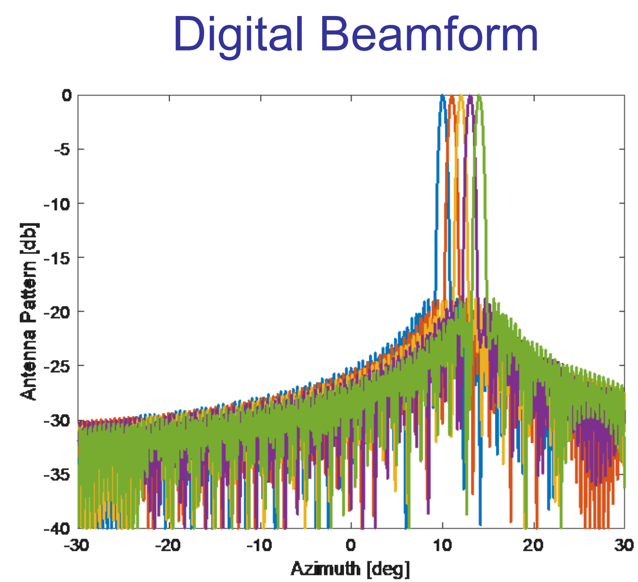

- A Narrow Band Signal Can Be Beam Steered With Phase Only Controls
- Wideband Array Requires A Combination Of Time Delay And Phase To Avoid Beam Squint During The Radar Operation
- Equalization Can Be Applied On Each Channel As Part Of Sidelobe Weighting

Multiple Channel Digital Beamforming Has Been Demonstrated On Commercially Available FPGA Processors

[aalf13]

Important Radar Waveform Relationships

- Range Resolution:
  - Waveform Bandwidth B
  - Grazing Angle To Image Surface γ_g
  - Weighting For Range Sidelobes k_R

$$\delta_R = \frac{k_R\, c}{2B \cos \gamma_g}$$

- Fractional Bandwidth
  - Ultra Wide Band If ΔB > 25 Percent

$$\Delta B = \frac{2(f_H - f_L)}{(f_H + f_L)}$$

- Cross-range (Azimuth) Resolution:
  - Valid For Center Wavelength λ_c
  - Depends On Integration Angle θ_I
  - Weighting For Cross-range Sidelobes k_{CR}

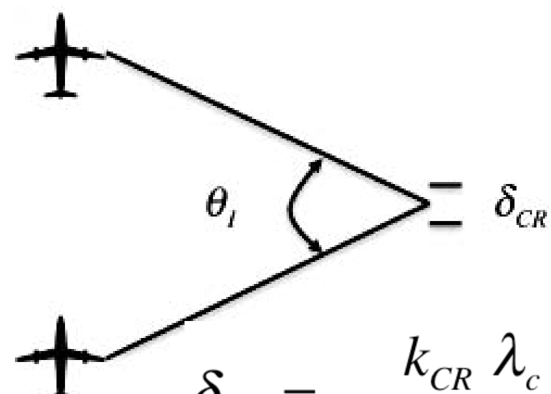

$$\delta_{CR} = \frac{k_{CR}\, \lambda_c}{4 \sin(\theta_I / 2)}$$

[carr95]

SAR Integration Angle

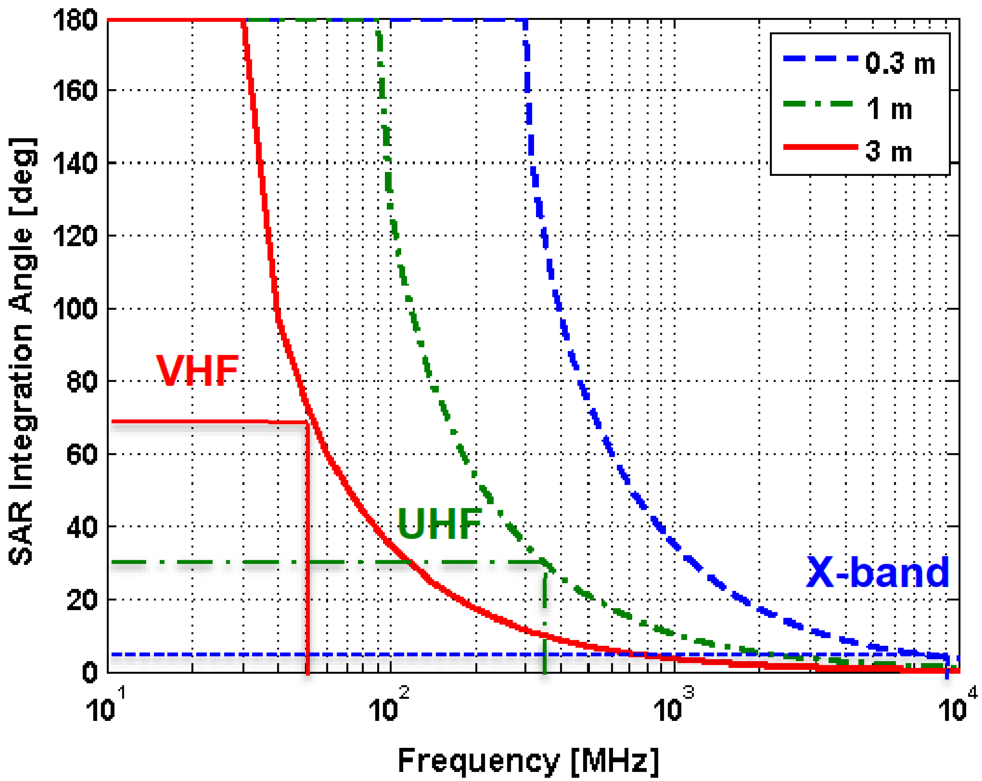

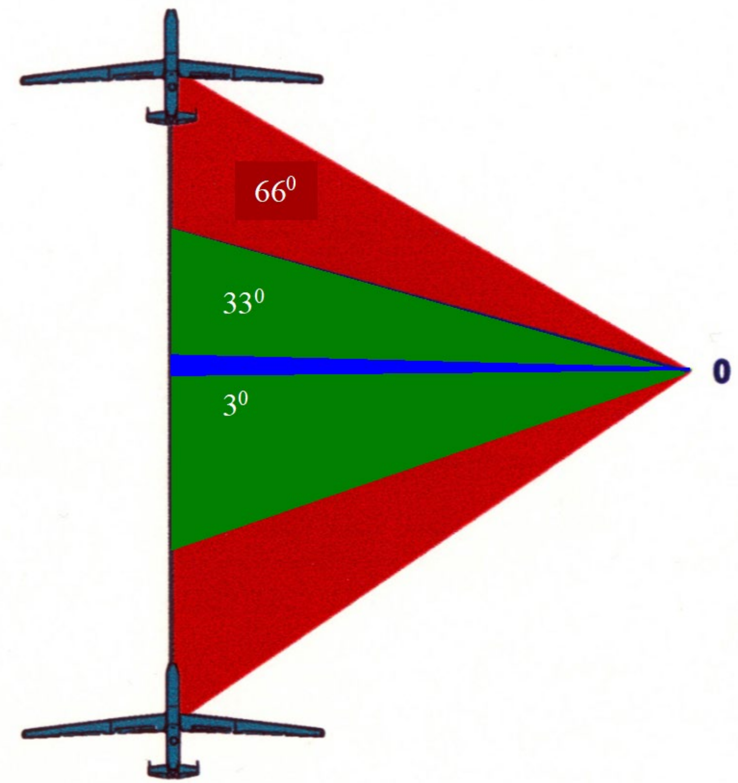

- Microwave Frequencies Have Most Efficient SAR Collection
- UWB Operation Requires Large Angles For Resolution
- Integration Times Depend On Platform Speed and Angle

[davi99]

UWB SAR Data Pulse Collection

Range Curvature

$$\Delta R_0 = \left[\frac{1}{\cos(\theta_I / 2)} - 1 \right] R_0$$

Number Range Bins

$$N_R = \frac{(W_S + \Delta R_0)}{\delta_R}$$

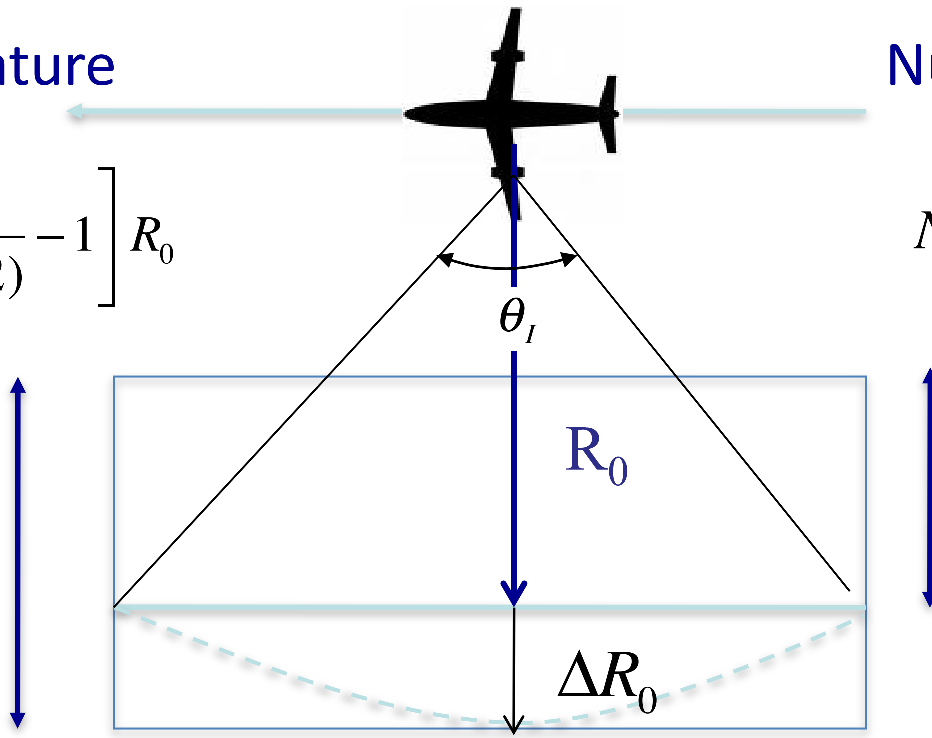

Input Range Swath

W_S - Output Range Swath

Along Track

Number of Pulses

$$N_P = \frac{k_S\, R_C\, \lambda_c}{2\, \delta_{CR}^2}$$

k_S -- Oversample ratio for data collection
R_C -- Range to swath center
λ_C -- Wavelength at center of band
δ_{CR} -- Cross-range resolution.

[davi11]

Additional Swath Width vs Integration Angle

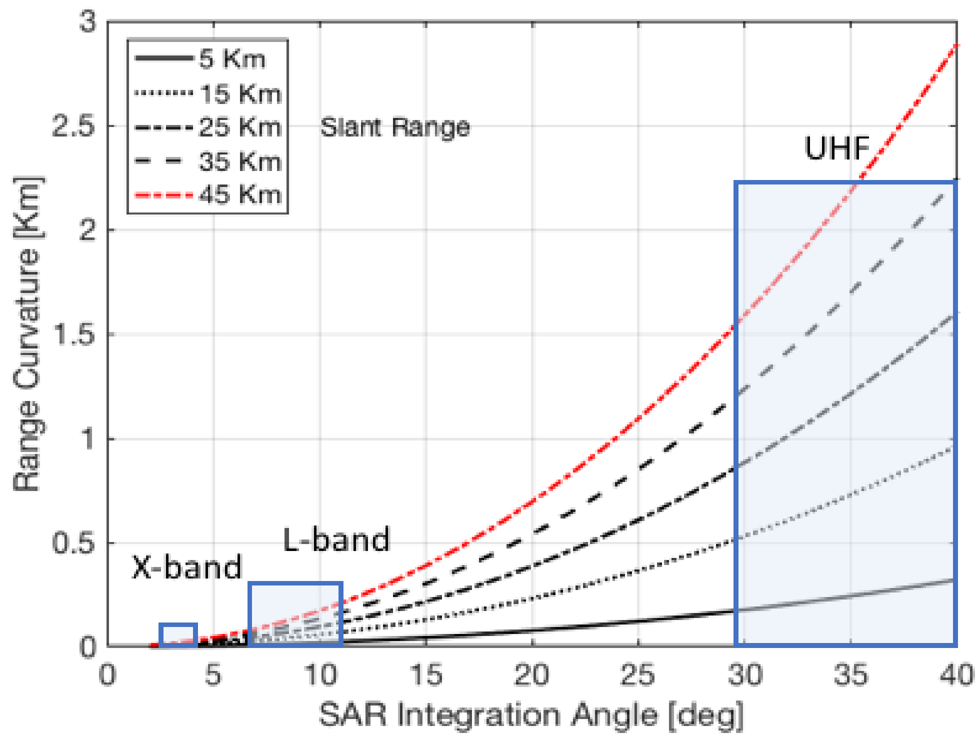

- Significant Range Curvature Experienced in UWB SAR Image Formation
  - UHF Image ~ 0.5 Km to 1.0 Km Cross Range Resolution
  - L-band Image ~ 2.0 Km to 3.0 Km Cross Range Resolution
- Range Curvature Not As Significant In Microwave SAR, A Little Extra Data

[davi11]

Range Curvature – UHF vs L-band SAR

SAR Fast Time Return | Range Compressed

UHF SAR Image

f_c = 400 MHz

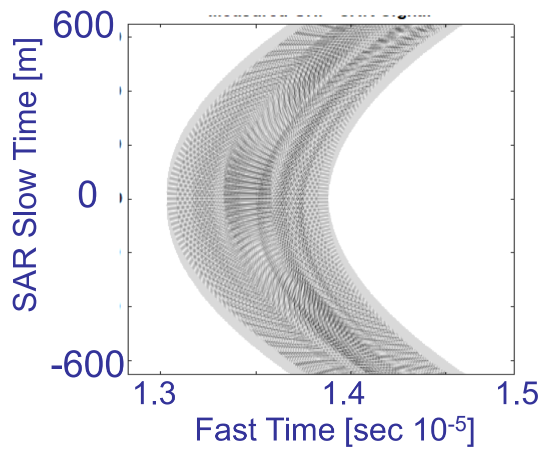

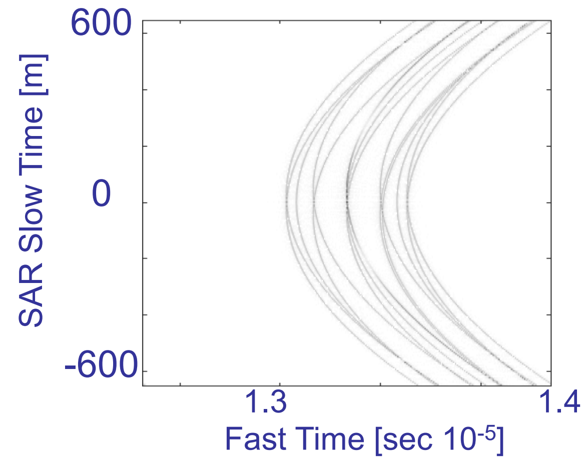

L-band SAR Image

f_c = 1400 MHz

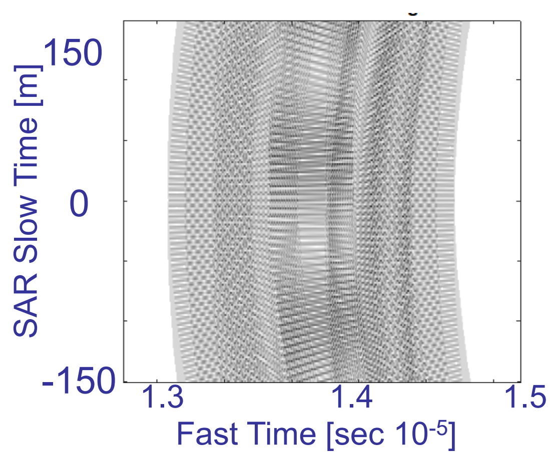

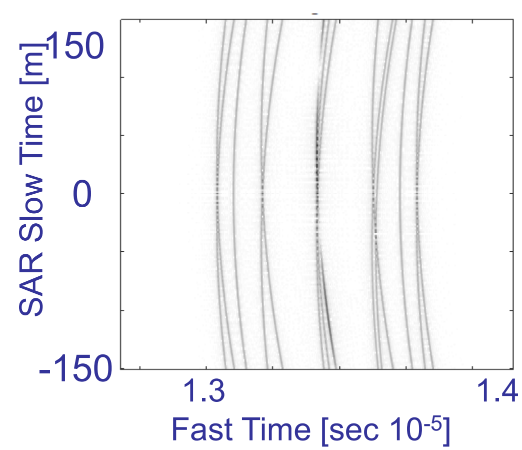

- Integration Angle And Range Curvature Difference Illustrated At Two SAR Frequencies

[davi21]

SAR Images For Geoscience Applications

160MHz X-Band SAR

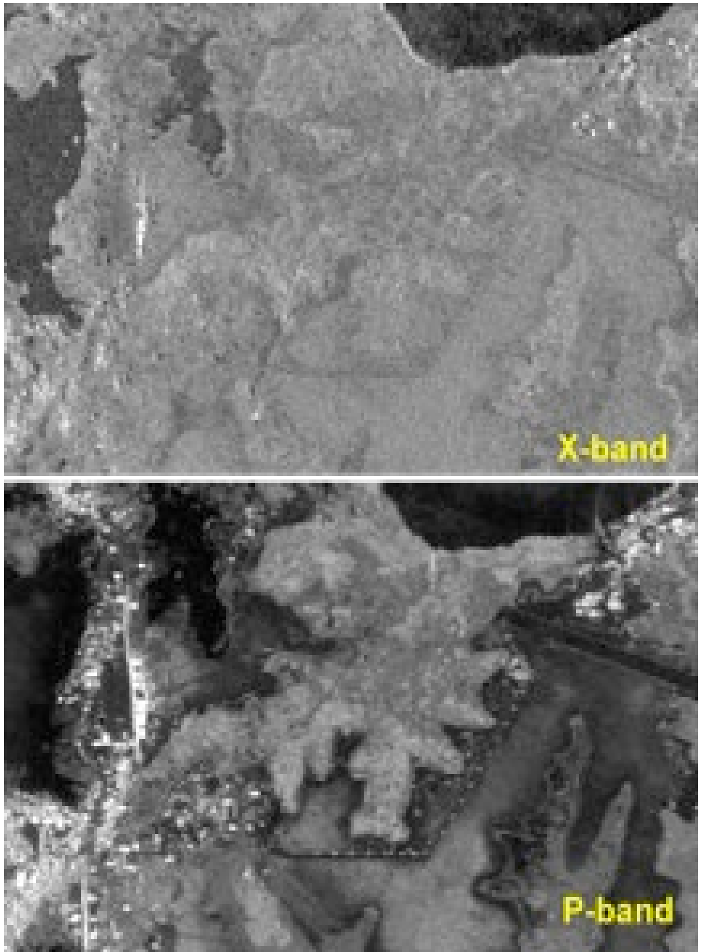

160MHz P-Band SAR

P-Band Transmit Spectrum

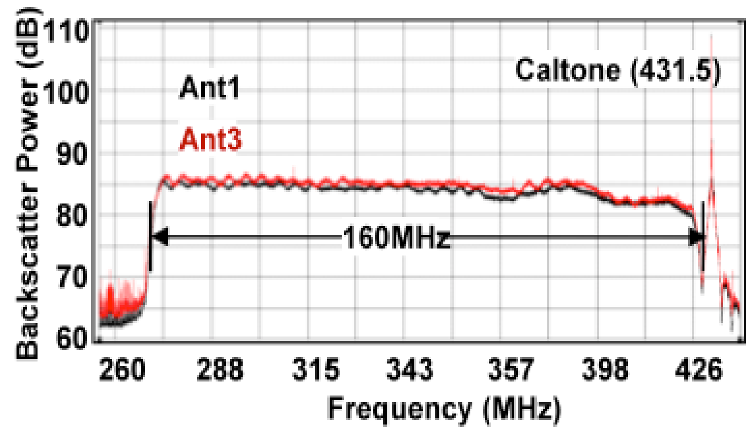

P & X-Band Impulse Response

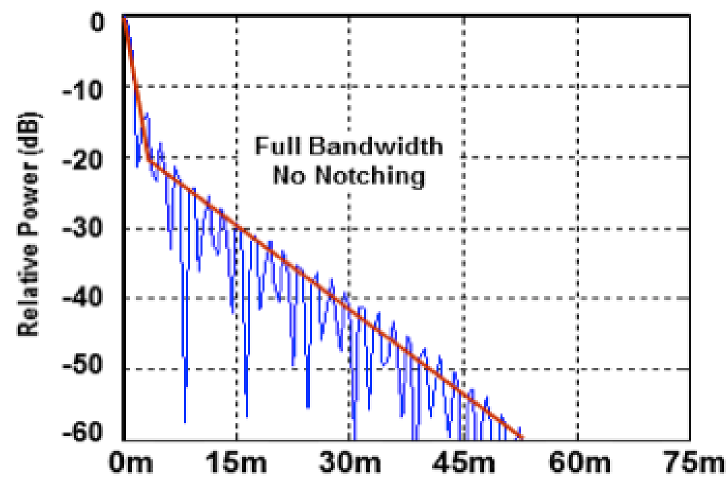

[davi15B]

Dual-Frequency GeoSAR Interferometric SAR

GeoSAR Application Results

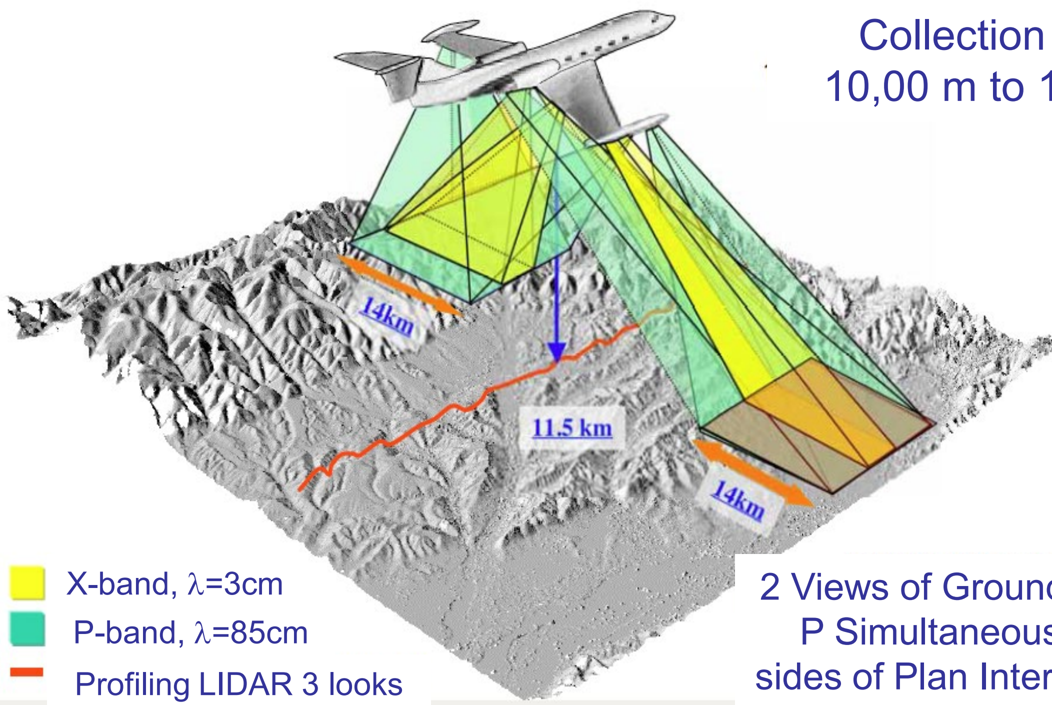

Collection Height
10,00 m to 12,500 m

X-band, λ=3cm
P-band, λ=85cm
Profiling LIDAR 3 looks

2 Views of Ground In X and P Simultaneously Both sides of Plan Interferometric

- GeoSAR Has The Capability To Collect Two Bands Of Interferometric SAR Data Out Of Both Sides Of The Gulfstream Aircraft
- By Using Both The X And P-band Imagery And DEM, The Image Processing Will Provide A Representation Of Bare Earth

[reis05]

Cross Track Interferometry Geometry

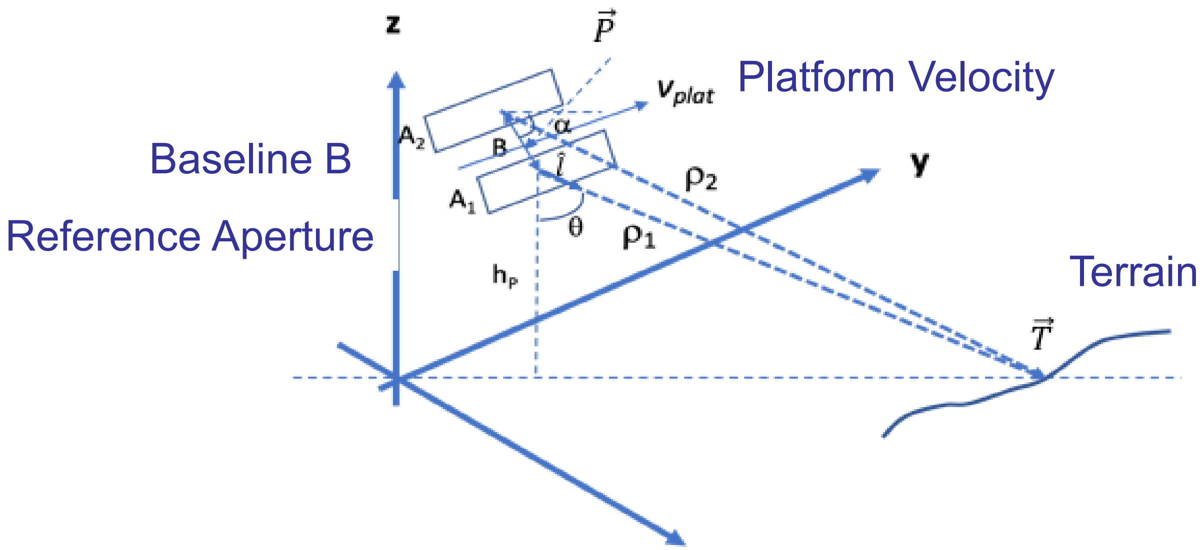

- A Baseline B Is Defined By The Location And Orientation Of The Two Antennas During The SAR Collection
- The Scattering Position On The Earth Is Obtained By The Vector $\vec{T}$,

$$\vec{T} = \vec{P} + \rho_i \hat{l}$$

  - Where A Reference Position One Of The SAR Antennas $\vec{P}$
  - And The Unit Look Vector $\hat{l}$ Along The Distance ρ_i (i = 1 or 2)
- As The Aircraft Moves Along The SAR Path, The Terrain Height Is Measured Through The Variation Of The Interferometric Phase Between The Two Antenna Phase Centers To Each Position On The Earth Surface

[rose00]

GeoSAR DEM at X and P-band In Colombia South America

X-band Image

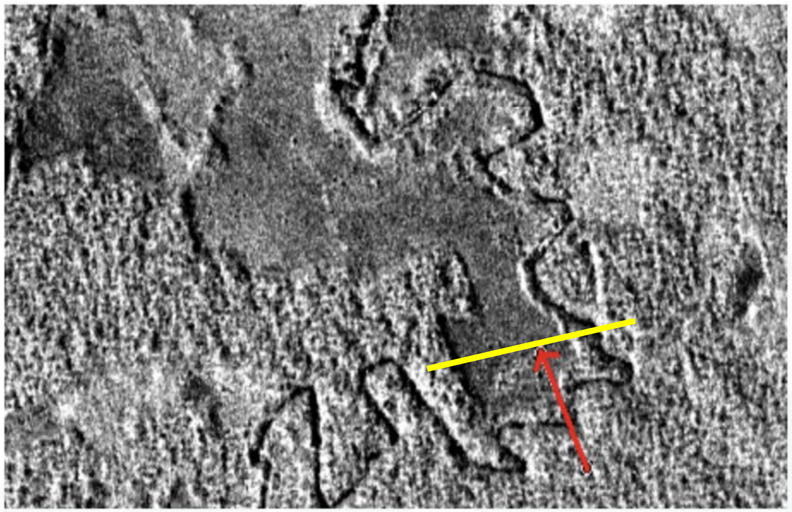

P-band Image

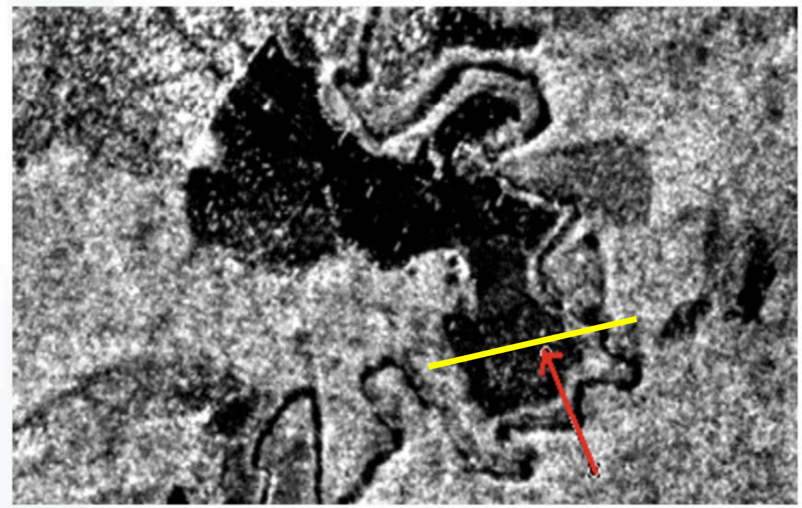

Spatial Profile for P-band DEM

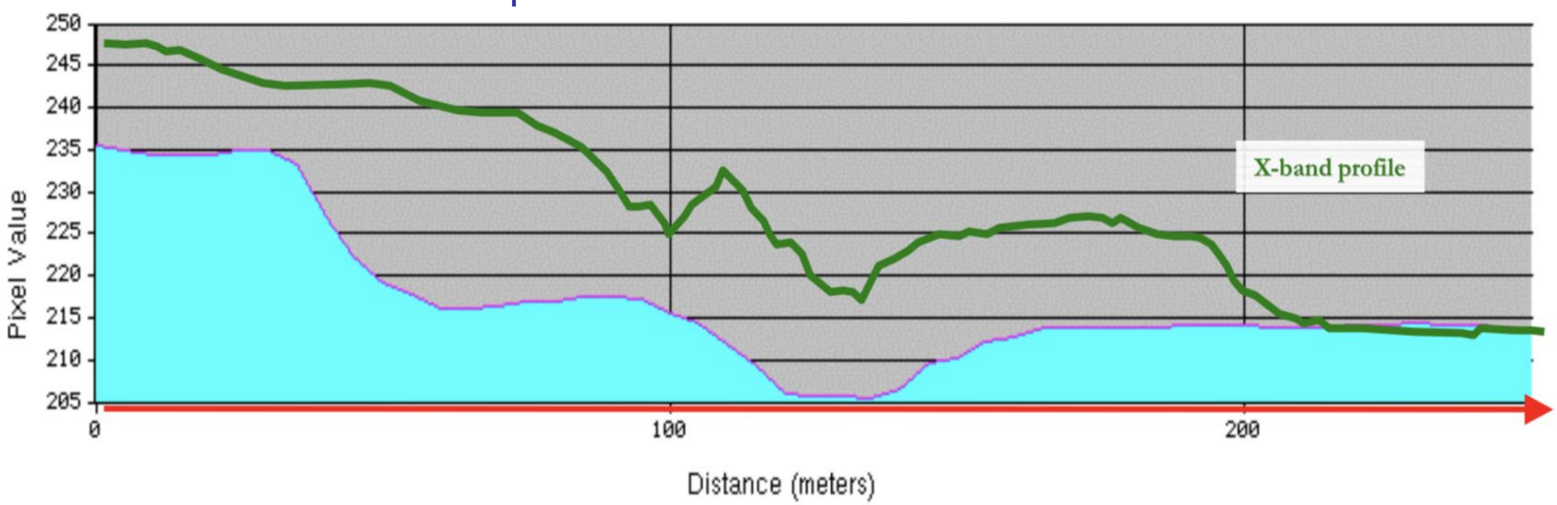

[reis05]

Wide Area Surveillance - GMTI

Wide Area Surveillance Geometry

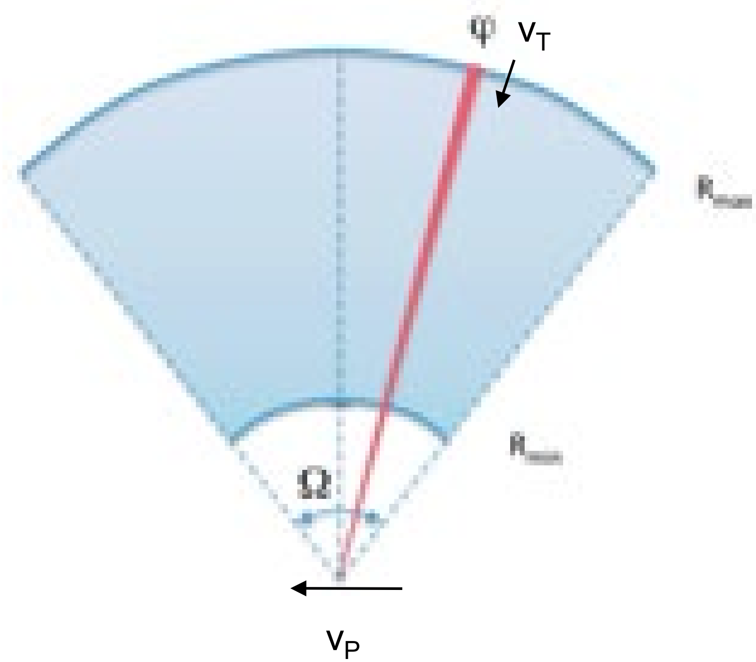

Moving Target Detection

$$v_T \geq v_P \sin\left(\frac{k\lambda}{2D}\right)$$

Area Coverage Rate

$$ACR_{GMTI} = \frac{\left(R_{max}^2 - R_{min}^2\right)}{2\ CPI}\varphi$$

- Moving Platform Causes Clutter To Spread Across Beamwidth
- Target Radial Velocity v_T Needs To Be Greater Than Clutter Spread
- Critical Figure of Merit –> Area Coverage Rate (ACR)
  = Footprint Area / Coherent Processing Interval (CPI)

Ground Moving Target Indication Radar

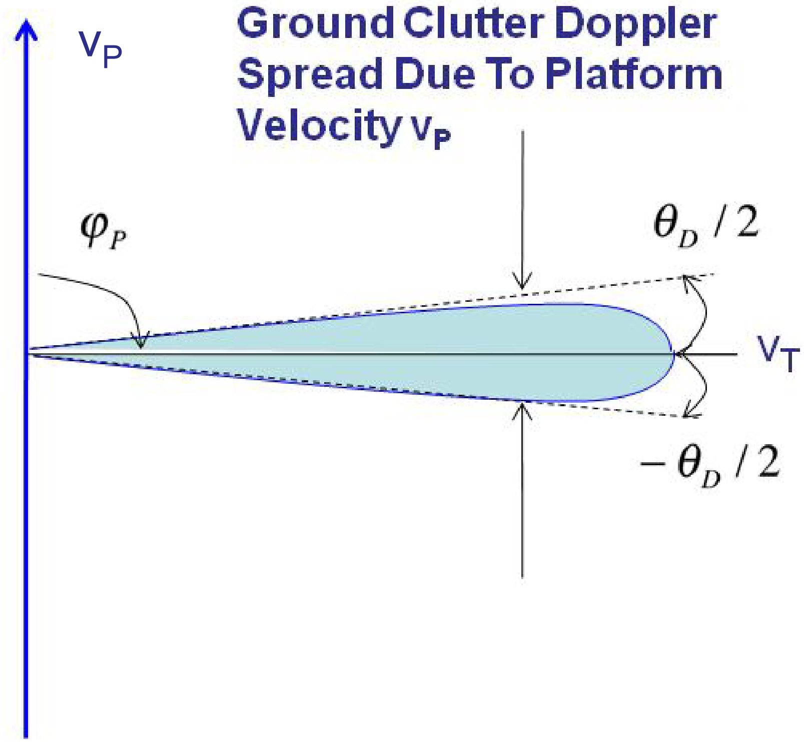

Ground Clutter Doppler Around Platform

$$f_{DP} = -\frac{2v_P}{\lambda}\cos(\varphi_P)\cos(\gamma_P)$$

Where φ_P is the angle from v_P
And γ_P is the grazing angle

The Beamwidth θ_D and associate clutter Spread is given by:

$$\theta_D = \frac{k\lambda}{D}$$

To Detect a Target with Velocity v_T it has to have a Doppler Greater than the half beamwidth $\theta_D / 2$ (with MTI Processing) or full beamwidth θ_D with no clutter processing

$$v_T \geq v_P \sin\left(\frac{k\lambda}{2D}\right)\cos(\gamma_P) \qquad \text{(With MTI Processing)}$$

[davi11]

Ground Moving Target Indication

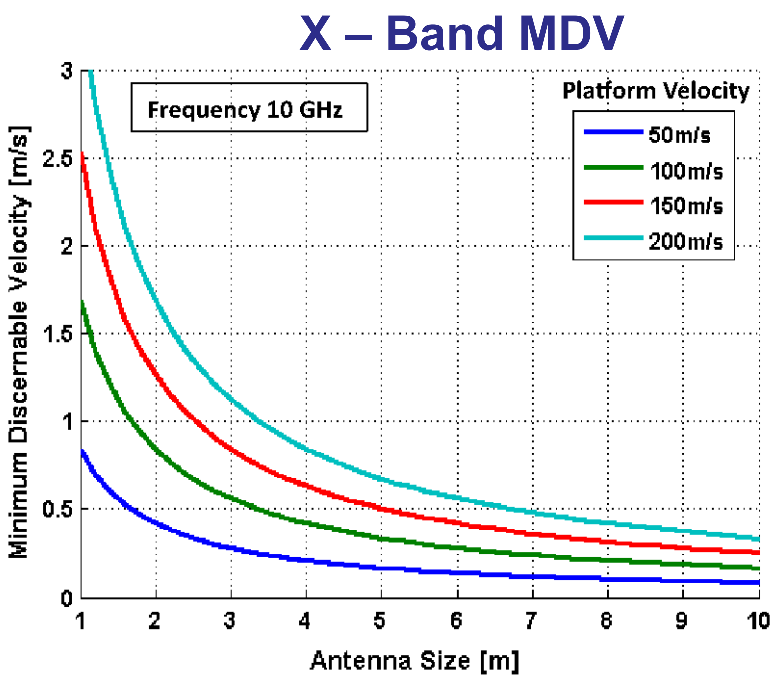

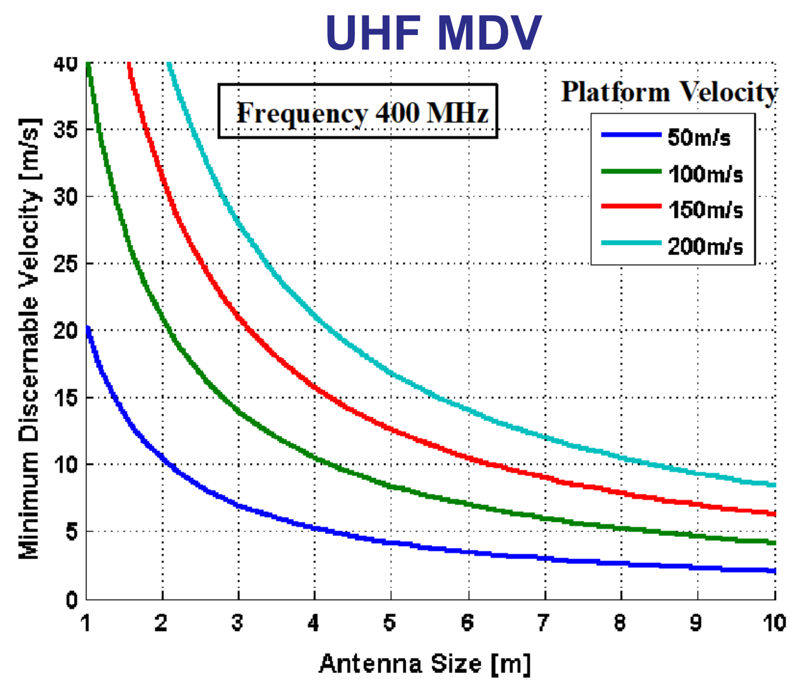

- Microwave Frequencies Enables Slow Moving Target Detection
  - Minimizes Beamwidth With Moderate Antenna Lengths
- UHF Long Wavelength Creates Difficulties For Effective Ground Moving Target Indication (GMTI) Radar
  - Excessively Large Antenna Needed For Low MDV
- Advanced Signal Processing Techniques
  - Space Time Adaptive Processing or Along Track Interferometry

[davi11]

Space Time Adaptive Processing (STAP)

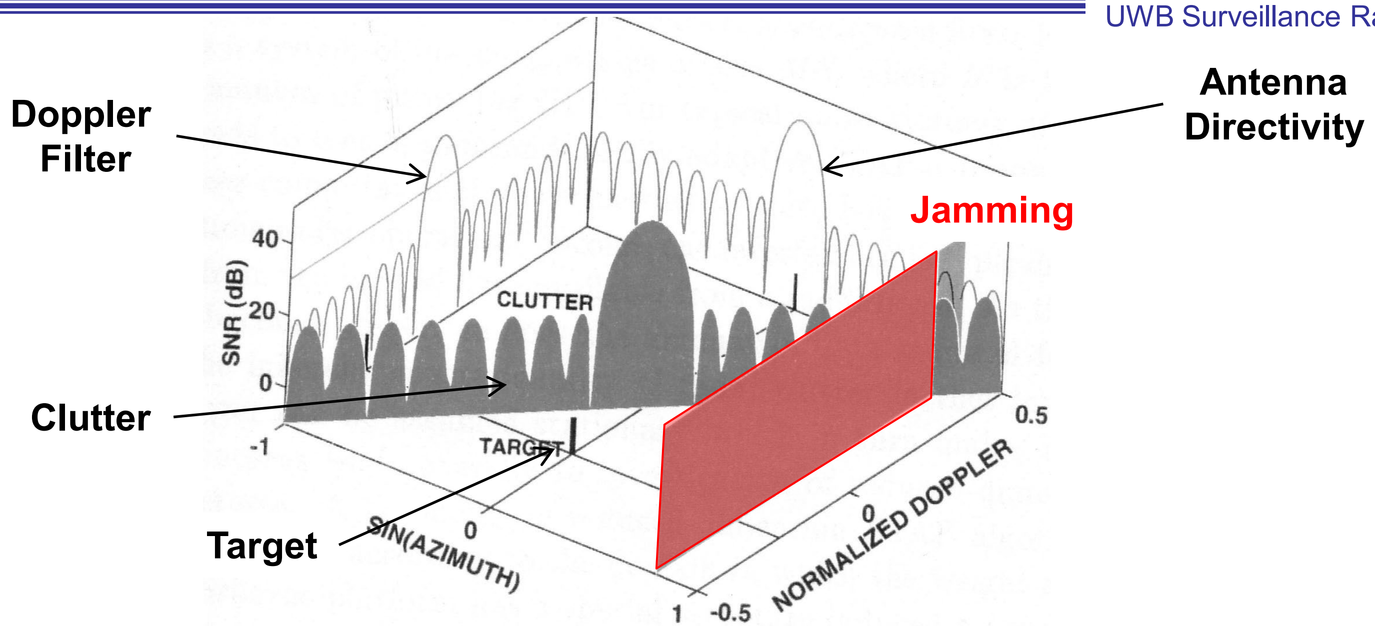

- GMTI Systems Are Integrated On Airborne Platforms,
  - Clutter Return Determined By The Antenna Directivity
  - Range And Doppler Characterized By The Waveform.
- STAP Combines The Signals Received From:
  - Multiple Elements Of An Antenna Array (The Spatial Dimension)
  - Multiple Pulse Repetition Periods (The Temporal Dimension)
- Both The Mainbeam And The Sidelobes Of The Antenna Affect The Minimum Detectable Velocity (MDV)

[ward94]

GMTI Clutter Spread with Platform Velocity

V_P = 1 meter / sec. V_P = 50 meter / sec.

Clutter to Noise of GMTI Radar.

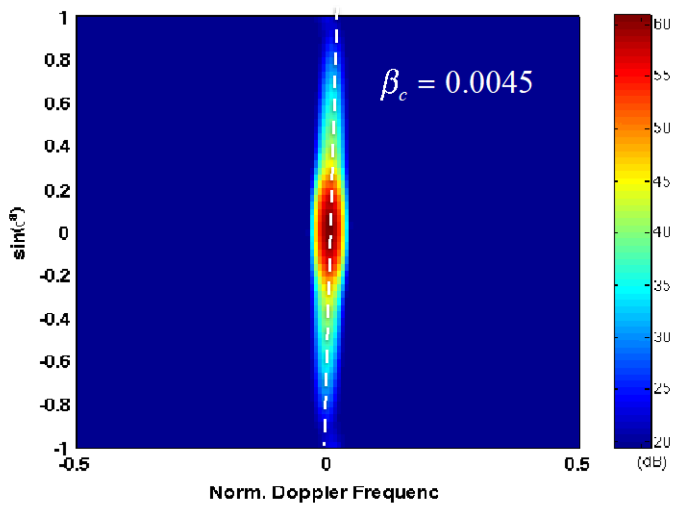

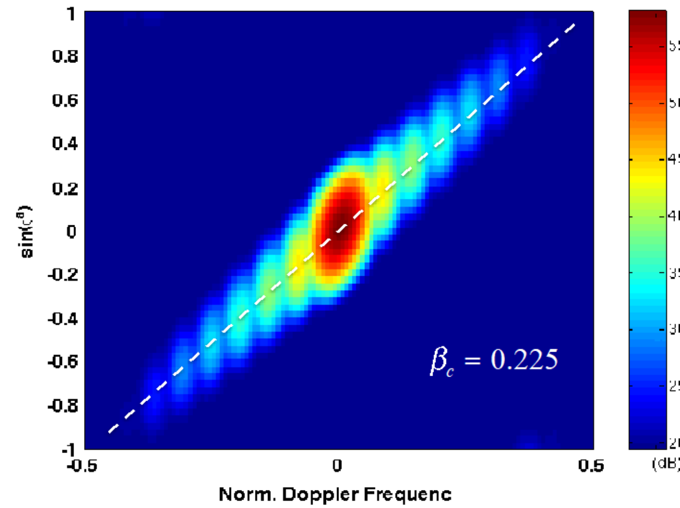

Signal to Interference Plus Noise From Ideal STAP

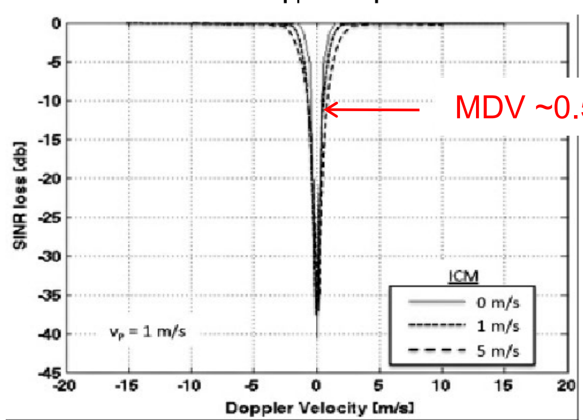

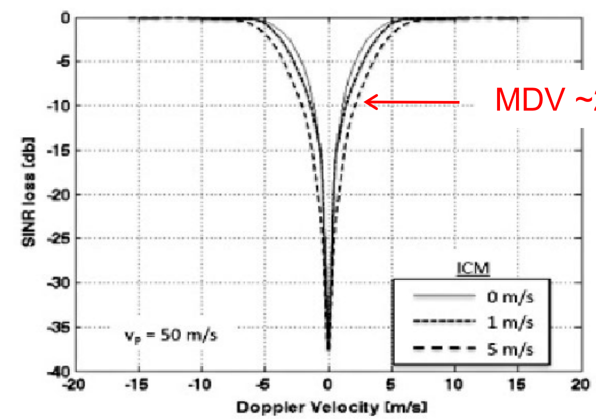

MDV Directly Affected By Clutter Spread With Platform Doppler, and Antenna/Waveform Sidelobes

[davi11]

Multiple Channel Radar with Sub-banding

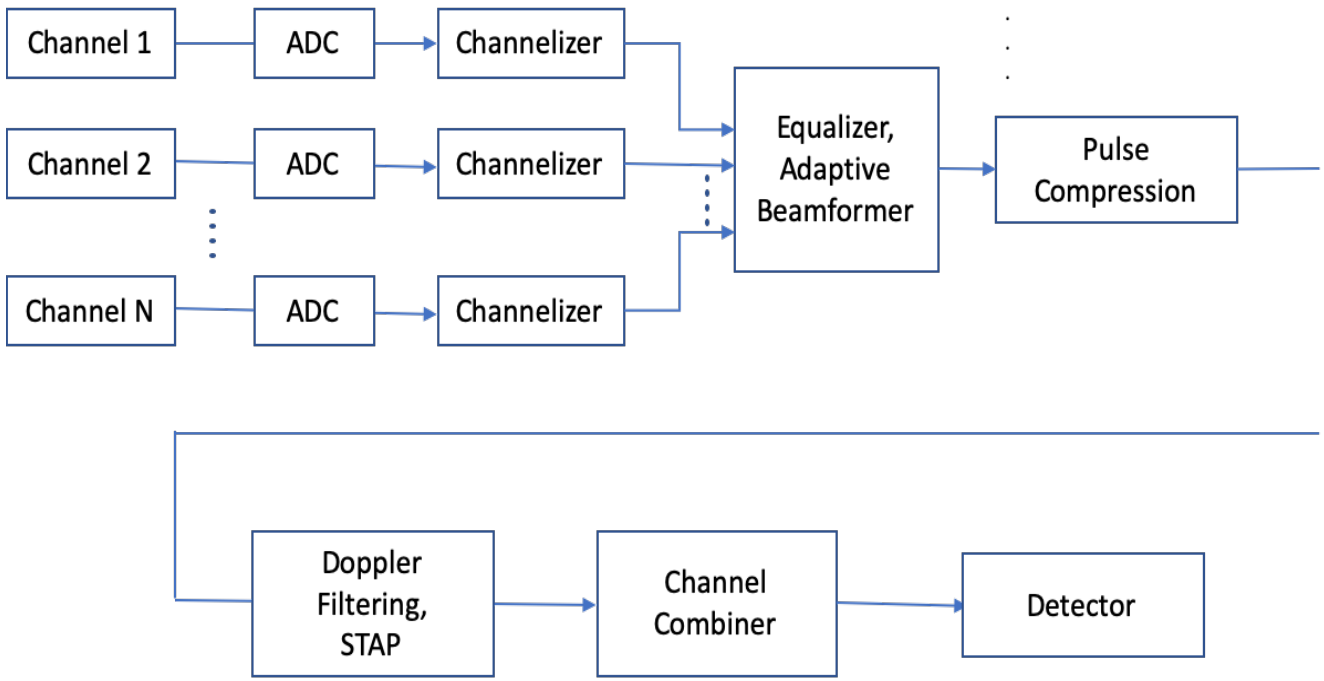

- A Modern Radar Has Multiple, Digitized Channels
- These Channels Need Sub-banding To
  - Channel Matching Amplitude and Phase
  - Handle The Processing Complexity
  - Maintain Coherence Or Channel Balance

[hoff00]

UWB STAP SINR Loss Reconstruction

STAP Sub-Band Processing

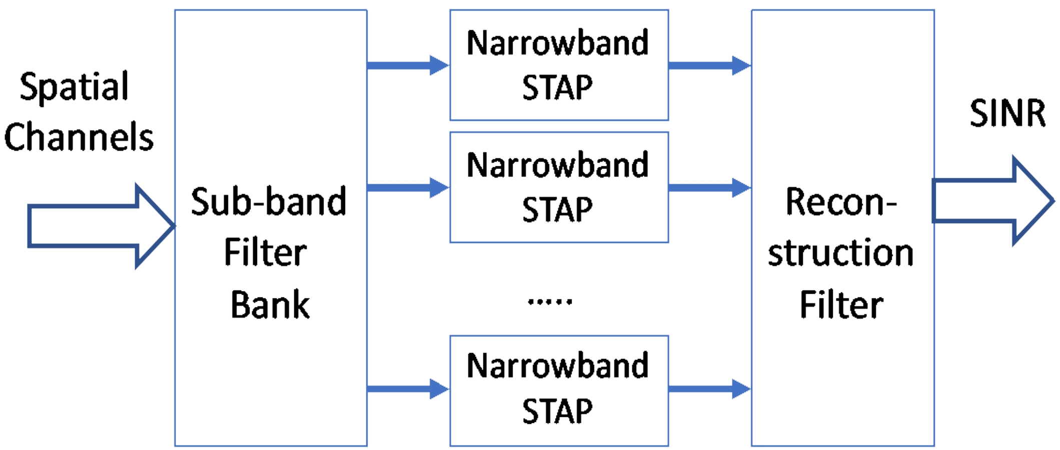

STAP MDV

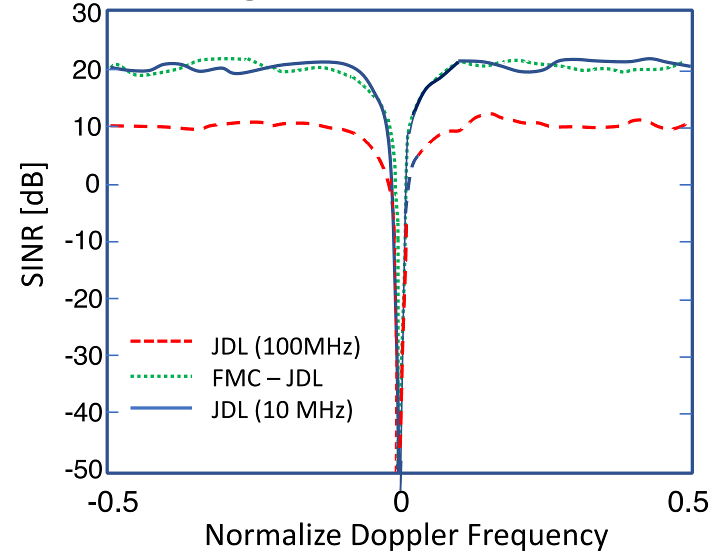

- Narrow Band STAP Has Efficient Detection Of Slow Moving Targets
- UWB STAP Suffers Significant Losses Due To Decorrelation Of The Independent Channels Due To Dispersion In Time And Doppler
- Losses Can Be Circumvented By Decomposing The Wideband Signal Into A Bank Of Narrow Sub-bands
- STAP Is Applied To Each Narrow Sub-bands, Followed By Recombining Into Wideband Signal For Targets After Clutter Suppression
- Losses Are Greatly Reduced, And MDV Is Maintained

[hime04]

Along-Track Interferometry for Slow Moving Target Detection

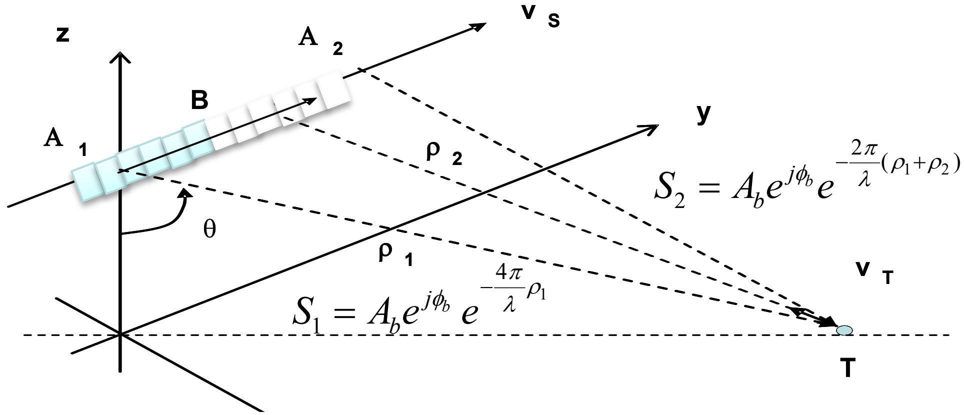

$$S_2 = A_b e^{j\phi_b} e^{-\frac{2\pi}{\lambda}(\rho_1+\rho_2)}$$

$$S_1 = A_b e^{j\phi_b} e^{-\frac{4\pi}{\lambda}\rho_1}$$

Theoretical ATI MDV Limit

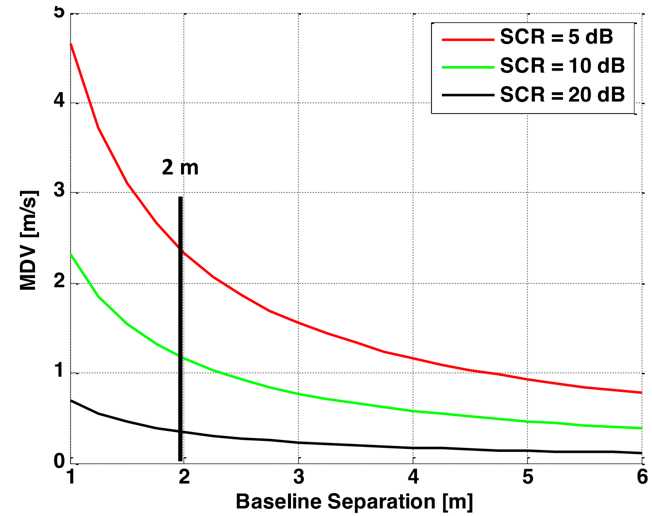

- Along-Track Separation Provides Phase Information $\Phi_{12} = \phi_2 - \phi_1$

$$= \frac{2\pi}{\lambda}\left[\rho_1(t) - \rho_2(t+\Delta t)\right] = \frac{2\pi}{\lambda} v_T \Delta t$$

- Phase change is related to radial velocity

$$v_r = \frac{\phi_{tgt}\lambda v_{plat}}{4\pi B}$$

- Minimal Discernable Velocity is a function of Along-Track Separation

$$\gamma = \frac{SNR}{SNR+1} \qquad \sigma_V = \frac{1}{\sqrt{2N_I}} \frac{\sqrt{1-\gamma^2}}{\gamma}\left(\frac{\lambda}{2\pi}\frac{v_{plat}}{B\sin(\theta)}\right)$$

- Along-Track Separation drives velocity ambiguities

$$v_{ambig} = \frac{\lambda v_{plat}}{B}$$

ATI Performance	
Baseline Separation	2 m
Unambiguous Radial Velocity	±22.5 m/s
Theoretical MDV Limit @ 20dB SCR	0.3 m/s

[kapf13]

Target Defocus Impact On Detection Accuracy

ATI Smear Loss vs Cross Range Resolution

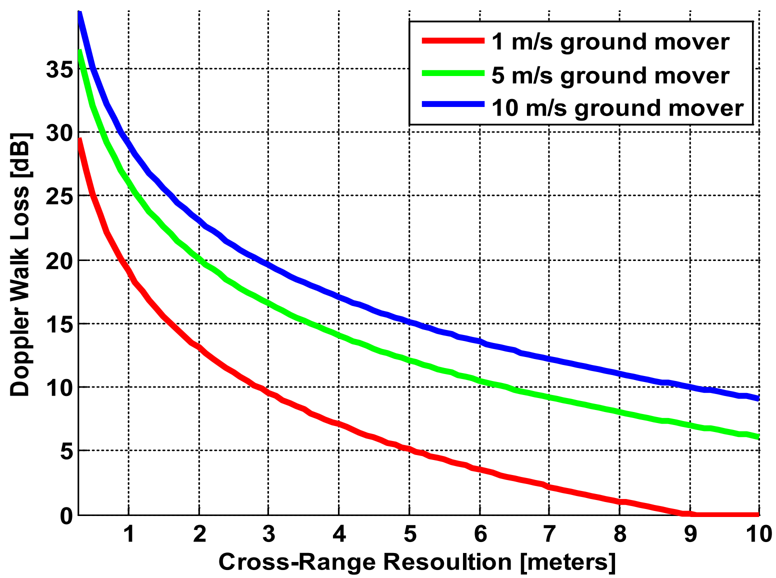

ATI Velocity Errors vs Target Radial Velocity

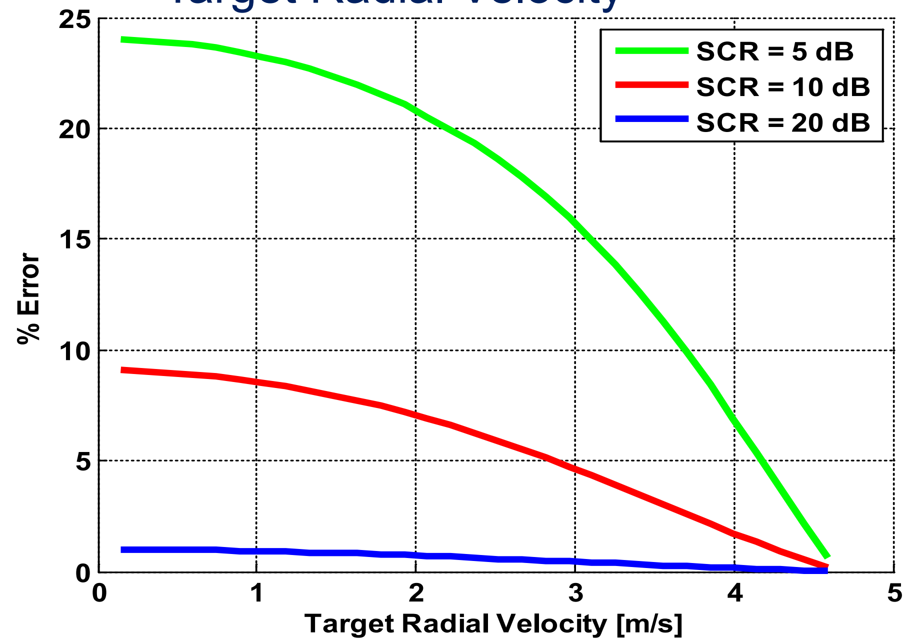

- ATI Of Moving Targets In SAR Image Before Focus
- Cross Range Resolution Requires Long Integration Times
  - Doppler Walk Increases With Target Velocity
- Defocus Of Targets Directly Affects Measurement of ATI Phase

Focus Before Detection Critical For UWB GMTI Operation

[kapf13] [chen04]

SAR/ATI Receiver Operating Characteristics

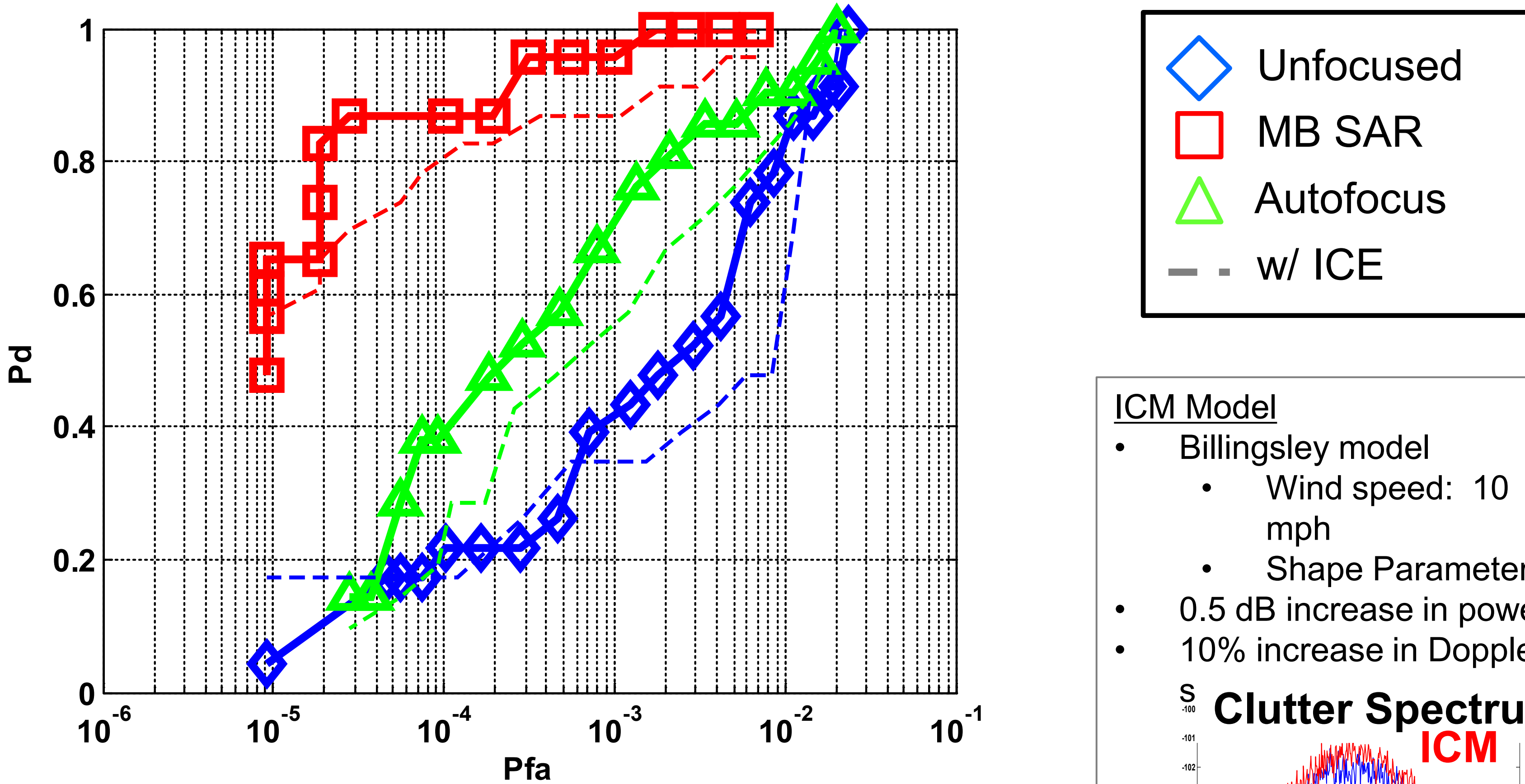

ICM Model

- Billingsley model
  - Wind speed: 10 mph
  - Shape Parameter: 8
- 0.5 dB increase in power
- 10% increase in Doppler s

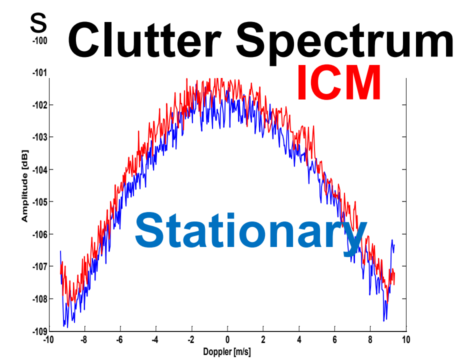

Intuitive Results, Focusing On Moving Targets Improve Coherent Integration In Back Projection, And With Improve Detection Performance.

[kapf13]

Summary

- UWB Radar Systems Have Been In Development For Over 40 Years – Primarily For Military Applications
- Commercial And Personal Communications Are Ubiquitous:
  - eCommerce Is The Major Source Of Many Businesses
  - Digital Communications Is Important For Security
- Adaptive Transmit and Receive Waveforms Required For Operation In Contested RF Environment
  - Cognitive Radio & Radar Technologies Developing
  - Machine Learning For Sparce Spectrum Access
- The International Radar Community Needs To Adapt And Develop New Technologies – Analogous To Cognitive Radio

References I

Reference	Authors	Title	Source
aalf13	David Aalfs	Adaptive Digital Beamforming	Principals of Modern Radar - Advanced Techniques, Chapt.9 Scitech Pub 2013
bani83	W. Banister, C.E Grove, J Song	Multibeam Antenna Development and Test Program	Final Report AFWAL-TR-3-1049, Contract F33615-79-C-1907 March 1983 AD078907
bark76	J. Barker, M.E.Davis	Ku-band Linear Phased Array	Microwave Journal, vol. 20, Oct. 1977, p. 44-57
bart05	Barton, D. K	*Radar System Analysis and Modeling*	Artech House, Norwood MA, 2005, pp. 94-99
bind95	B.T. Binder, M.F. Toups, S. Ayasli, EM. Adams	SAR Foliage Penetration Phenomenology of Tropical Rain Forest and Northen US Forest	Proc. 1995 IEEE International Radar Conference, Washington DC May 1995 p 158
brya00	T.G. Bryant, G.B. Morse, L.M. Novak, J.C. Henry	Tactical Radars for Ground Sureillance	Linclon Laboratory Journal, v. 12, no. 2, 2000, p 341
carr95	W.G. Carrara, R.S. Goodman, R.M.Majewski	Spotlight Sythetic Aperture Radar	Artech House, Norwood MA, 1995
chen04	C.W. Chen	Performance Assessment of Along-track Interferometry For Detecting Ground Moving Targets	Proc. 2004 IEEE Radar Conference, Philadelphia PA, April 2004
davi11	M.E.Davis	Foliage Penetration Radar - Detection and Characerization of Objects Under trees	Scitech Publishing, Raleigh NC, April 2011
davi15B	M.E. Davis, J.J. Reis	Operation of GeoSAR Foiage Penetration Modes in Spectrum Regulated Environment	Proc. 2015 IEEE Radar Conference, Pretoria South Africa, October 2015
davi21	M.E. Davis	Ultra Wideband Surveillance Radar	IET Publications, London UK, January 2011

Advancing Technology for Humanity

References 2

Reference	Authors	Title	Source
davi99	M.E. Davis, P.G. Tomlinson, R.P. Maloney	Technical Challenges in Ultra Wideband Radar Development for Target Detection and Terrain Mapping	Proc 1999 IEEE Radar Conference Boston MA April 1999 p 1
fant95	R.L. Fante	Multifrequency Detection of Slowly Fluctuating Targets	Unpublished MITRE Memo MTR 95B00021, Bedford MA, February 1995
hens07	Hensley, S., Madsen, S.N.,	Interferometric Radar Waveform Design and the Effective Interferometric Wavelength	Proceedings 2007 Waveform Diversity & Design Conference, Pisa Italy, June 2007
hime04	B Himed, K Kim, Y Zhand, A Haggari	A New Approach to Widband Space Time Adaptive Processing (W-STAP)	Proc. 2004 IEEE Sensor Array and Multichannel Signal Processing Workshop, Barcelona Spain, July 2004, pp. 672 - 676
hoff00	A Hoffman S.M.Kogon	Subband STAP in wideband Rdar Systems	Proc. 2000 IEEE International Radar Conference, Arlington VA, pp.256-60
kapf13	R.M.Kapfer, M.Pohl, M.E.Davis	Detection Improvement for UWB Along Track Interferometery of Moving Targets Under Foliage	Proc. 2013 IEEE Radar Conference, Atlanta GA, May 2013
reis05	Reis, J.J., Hensley, S.,	GeoSAR P-band and X-band Performance in Southern California and Colombia, South America	ISPRS International Workshop, Banff, Canada, June 2005
rose00	P.A. Rosen, S. Hensley, et.al	Synthetic Aperture Radar Interferometry	Proc IEEE, Vol. 88, No.3, March 2000, p.333-81
simk98	Simkins, W.L	Air Defense Initiative Clutter Model	Report AFRL-SN-RS-TR-1998-95 , PAR Corporation, New Hartford NY, April 1998, DTIC A346972
vanz97	Van Zyl, J.J., Chu, A., Hensley, S., Lou, Y. Kim, Y.J., Madsen, S.N.,	The AIRSAR/TOPSAR Integrated Multi-frequency Polarimetric and Interferometric SAR Processor	Proceedings 1997 IGARS Symposium, vol. 3, Singapore, 1997
ward94	J. Ward	Space Time Adaptive Processing for Airborne Radar	MIT Lincoln Laboratory Technical Report TR-1015, Lexington MA December 1994